VI International Conference on Computational Methods for Coupled Problems in Science and Engineering
COUPLED PROBLEMS 2015
B. Schrefler, E. Oñate and M. Papadrakakis(Eds)

BALLISTIC CHARGE TRANSPORT IN A TRIPLE-GATE SILICON NANOWIRE TRANSISTOR

O. MUSCATO, T. CASTIGLIONE AND C. CAVALLARO

Dipartimento di Matematica e Informatica
Università degli Studi di Catania
Viale A. Doria 6, 95125 Catania, Italy
e-mail: muscato@dmi.unict.it, castiglione@dmi.unict.it

Key words: Silicon nanowires, Schrödinger-Poisson-Boltzmann system, Variational Method, ballistic transport.

Abstract. In this paper we investigate the electrostatics and charge transport in a triple-gate Silicon Nanowire transistor. The quantum confinement in the transversal dimension of the wire have been tackled using the Schrödinger equation in the Effective Mass Approximation coupled to the Poisson equation. This system have been solved efficiently using a Variational Method. The charge transport along the longitudinal dimension of the wire has been considered using the semiclassical approximation, in the ballistic regime.

1 INTRODUCTION

Silicon nanowires (SiNW) are considered an interesting alternative architecture to the conventional planar technology for electronic devices, because different electronic structures and transport properties in one dimension can be utilized to fabricate high performance and highly packed integrated circuits. By shrinking the cross-section of SiNW electronic devices, effects of quantum confinement are observed and the wave nature of the electrons must be taken into account. In addition, it is well known that the behavior of field-effect transistors is dominated by electrostatics, which has therefore to be accurately simulated in order to reproduce the device electrical behavior. In order to accurately model transport charge in SiNW one have to take into account its transversal and longitudinal dimensions. For nanowires with transversal dimensions greater than 5 nm, the 2D Schrödinger equation in the Effective Mass Approximation (EMA) represents a good approximation to describe the quantum confinement [1], but below, atomistic electronic structure models must be employed. For longitudinal lengths (called channel) greater than 20nm, the charge transport can be described with a semiclassical scheme, in which the charges are treated as newtonian particles. Below this channel dimension, quantum mechanical simulations based on the nonequilibrium Greens function (NEGF) formalism

are mandatory. The goal of this paper will be the investigation of the charge transport in a triple-gate SiNW transistor within the effective mass approximation, in the semiclassical regime. The EMA equation will be solved with a Variational Method, with the main advantage to eliminate discretization errors as well as to cut down computational time with respect to a purely-numerical approach. The charge transport along the channel will be tackled in a ballistic regime.

2 Transport equations

In the following we shall consider a SiNW with rectangular cross section. For a quantum wire with longitudinal expansion in z-direction, and confined in the plane x-y, the normed electron wave function $\psi(x,y,z)$ can be written in the form

$$\psi(x,y,z) = \chi_\alpha(x,y)\frac{e^{ik_z z}}{\sqrt{L_z}} \tag{1}$$

where $\chi_\alpha(x,y)$ is the wave function of the α-th subband and the term $e^{ik_z z}/\sqrt{L_z}$ describes an independent plane wave in z-direction confined to the normalization length, where $z \in [0, L_z]$ and k_z is the wave vector number. In general the electron is subject to external confining potential U, such as by a discontinuity in the band gap at an interface between two materials, and also to the effect of the other electrons in the system. The simplest approximation, called *Hartree approximation*, is to assume that the electrons as whole produce an average electrostatic energy potential, and that a given electron feels the resulting total potential V_{tot}

$$V_{tot}(x,y,z) = U(x,y) - e\Phi(x,y,z) \quad . \tag{2}$$

The normed wave function satisfies the Schrödinger equation in the Effective Mass Approximation, i.e.

$$\left[-\frac{\hbar^2}{2m^*}\Delta + V_{tot}(x,y,z)\right]\psi = E\,\psi \tag{3}$$

where E is the total energy, and m^* denotes the effective mass of the electron in the conduction band. By inserting eq.(1) into eq.(3), in each z-th cross section of the device, one obtains the following equation for the envelope function $\chi_{\alpha z}(x,y)$

$$\begin{cases} H\chi_{\alpha z} = \varepsilon_{\alpha z}\chi_{\alpha z} \\ H = \left[-\frac{\hbar^2}{2m^*}\left(\frac{\partial^2}{\partial x^2} + \frac{\partial^2}{\partial y^2}\right) + V_{tot}(x,y,z)\right] \\ E_{\alpha z} = \varepsilon_{\alpha z} + \frac{\hbar^2 k_z^2}{2m^*} \end{cases} \tag{4}$$

where $\varepsilon_{\alpha z}$ is the kinetic energy associated to the confinement in the x-y plane, and we have assumed the parabolic band approximation. The term Φ satisfies the Poisson equation

$$\nabla\cdot[\epsilon\nabla\Phi(x,y,z)] = e(n - N_D + N_A) \tag{5}$$

where N_D, N_A are the doping profile (due to donors and acceptors) and $n(x,y,z,t)$ is the electron density, which depends on $\chi_{\alpha z}$

$$n(x,y,z,t) = \sum_{\alpha} \rho^{\alpha}(z,t)|\chi_{\alpha z}(x,y,t)|^2 \tag{6}$$

where ρ^{α} is the subband linear density in the z-direction

$$\rho^{\alpha}(z,t) = \frac{2}{2\pi}\int f_{\alpha}(z,k_z,t)dk_z \tag{7}$$

f_{α} being the electron distribution function in the α-subband. For an assigned confining potential, one has to solve a coupled problem formed by the eqs.(4), (5) and (6) to find $\varepsilon_{\alpha z}, \chi_{\alpha z}$ in each cross-section. The subband electron distribution function can be obtained by solving the 1-D Multiband Boltzmann Transport Equation (MBTE), which forms an integro-differential system in two dimensions in the phase-space and one in time, with a complicate collisional operator. The full solution of the MBTE can be obtained or by using cpu-demanding methodologies such as the Monte Carlo one [2]-[10] or deterministic numerical solvers [11],[12],[13], or by introducing hydrodynamic models [14]-[18].

3 Solution of the EMA equation

For a fixed total potential $V_{tot}(x,y,z)$ in each cross-section (with z= const.) one has to solve the eigenvalues problem (4). This can be achieved or by using a finite difference numerical scheme, or by using a Variational Method. With a finite difference scheme, a 2D spatial mesh with N_1 grid points in the x-dimension and N_2 in y-dimension is introduced. If we approximate the differential operator $\frac{\partial^2}{\partial x^2}$ with a central difference formula, then the eigenvalues problem (4) reduces to a system of linear equations having a $N_1 \times N_2$ matrix. The discretization error, in this case, is quadratic in the mesh size [19].

With the Variational Method [20], the eigenvalue problem of the Hamilton operator H is approximated by the eigenvalue problem of the matrix $\mathcal{H}$

$$\mathcal{H}\mathbf{v} = \lambda\mathbf{v} \quad , \quad \mathcal{H}_{\{i\}\{j\}} = \left\langle \psi_{\{i\}}|H|\psi_{\{j\}}\right\rangle \quad , \quad \mathbf{v} = (v^1, v^2, ...) \tag{8}$$

where the matrix elements $\mathcal{H}_{\{i\}\{j\}}$ are expectation values of the Hamilton operator H with respect to a set of orthonormal functions $\{|\psi_{\{1\}}\rangle, |\psi_{\{2\}}\rangle, ...\}$ which span the Hilbert space of H. Then the α-th approximated eigenvalue of the Hamilton operator H is the α-th eigenvalue of the matrix $\mathcal{H}$ i.e. $\varepsilon_{\alpha} \simeq \lambda_{\alpha}$, and the α-th eigenfunction χ_{α} of the Hamilton operator H is approximates as

$$\chi_{\alpha} \simeq \sum_{\{i\}} v_{\alpha}^{\{i\}} \, |\psi_{\{i\}}\rangle \quad . \tag{9}$$

We observe that the number of the orthonormal functions that span the Hilbert space of H is infinite. Since the number of used orthonormal functions is finite, the solutions of

$\mathcal{H}$ span in general a subspace of H. Hence the variational method is only an advantage if the set of orthonormal functions is chosen appropriately so that the matrix elements $\mathcal{H}_{\{i\}\{j\}}$ are easily calculable and the accuracy of the approximation can be ensured for a small number of orthonormal functions. A good choice for a set of orthonormal functions are the eigenstates of the two-dimensional anisotropic harmonic oscillator which are given by

$$|\psi_{j_x,j_y}\rangle = \frac{(ab)^{\frac{1}{4}}}{\sqrt{\pi 2^{j_x+j_y} j_x! j_y!}} \exp\left(-\frac{ax^2}{2} - \frac{by^2}{2}\right) H_{j_x}(\sqrt{a}x) H_{j_y}(\sqrt{a}y) \tag{10}$$

$$a = \frac{m^*\omega_x}{\hbar} \quad , \quad b = \frac{m^*\omega_y}{\hbar} \quad , \quad \{j\} = (j_x, j_y) \in \mathbb{N} \times \mathbb{N} \tag{11}$$

where j_x, j_y are the quantum numbers, $H_{j_x}(\sqrt{a}x)$ is the Hermite polynomial of order j_x and ω the angular velocity. Then, the elements of the matrix $\mathcal{H}_{\{i\}\{j\}}$ are formed by two contributions:

$$\mathcal{H}_{\{i\}\{j\}} = \mathcal{H}^{(1)}_{\{i\}\{j\}} + \mathcal{H}^{(2)}_{\{i\}\{j\}} = \left\langle \psi_{\{i\}} \left| -\frac{\hbar^2}{2m^*}\left(\frac{\partial^2}{\partial x^2} + \frac{\partial^2}{\partial y^2}\right) \right| \psi_{\{j\}} \right\rangle + \left\langle \psi_{\{i\}} | V_{tot} | \psi_{\{j\}} \right\rangle \quad . \tag{12}$$

The first term can be evaluated as:

$$\mathcal{H}^{(1)}_{\{i\}\{j\}} = \frac{\hbar\omega_x}{4}\delta_{i_y,j_y}\left[(2j_x+1)\delta_{i_x,j_x} - \sqrt{j_x^2 - j_x}\,\delta_{i_x,j_x-2} - \sqrt{i_x^2 - i_x}\,\delta_{i_x-2,j_x}\right] + \frac{\hbar\omega_y}{4}\delta_{i_x,j_x}\left[(2j_y+1)\delta_{i_y,j_y} - \sqrt{j_y^2 - j_y}\,\delta_{i_y,j_y-2} - \sqrt{i_y^2 - i_y}\,\delta_{i_y-2,j_y}\right] \quad . \tag{13}$$

The second term depends on $V_{tot}(x, y, z)$. Let us suppose that this term reduces to a two-dimensional finite rectangular potential well $U(x, y)$, i.e.

$$U(x,y) = \begin{cases} 0 & \forall (x,y) \in [-L_x/2, L_x/2] \times [-L_y/2, L_y/2] \\ U_0 & \text{otherwise} \end{cases} \tag{14}$$

where the depth of the potential well is usually taken U_0 = -4.05 eV (the work function of Si) and L_x and L_y are the lengths of the well in x and y direction respectively. In this case, after some calculations, we have

$$\mathcal{H}^{(2)}_{\{i\}\{j\}} = \frac{U_0}{\pi}\sqrt{\frac{1}{2^{i_x+i_y+j_x+j_y} i_x! i_y! j_x! j_y!}} \exp\left[-\frac{1}{4}\left(aL_x^2 + bL_y^2\right)\right] \times \left\{\sum_{k=0}^{\min(i_x,j_x)} 2^k k! \binom{i_x}{k}\binom{j_x}{k}\left[H_{i_x+j_x-2k-1}(-\sqrt{a}L_x/2) - H_{i_x+j_x-2k-1}(\sqrt{a}L_x/2)\right]\right\} \times \left\{\sum_{k=0}^{\min(i_y,j_y)} 2^k k! \binom{i_y}{k}\binom{j_y}{k}\left[H_{i_y+j_y-2k-1}(-\sqrt{b}L_y/2) - H_{i_y+j_y-2k-1}(\sqrt{b}L_y/2)\right]\right\} \tag{15}$$

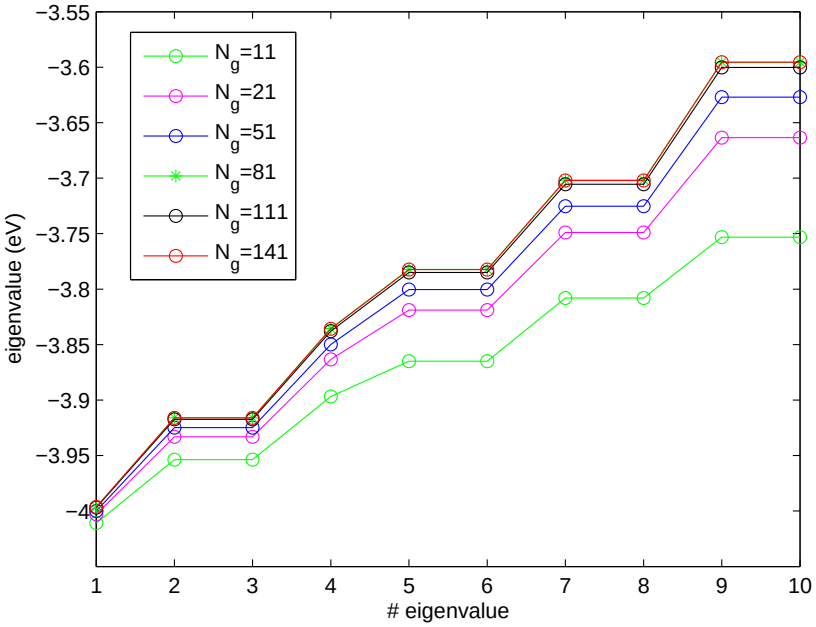

Figure 1: The subband energies ε_α (4) obtained with a finite difference solver, with N_g grid points in each axes.

If $j_x = 0, 1, ..., N_x$ and $j_y = 0, 1, ..., N_y$ then the matrix $\mathcal{H}$ has $(N_x + 1)(N_y + 1)$ rows and columns. The main advantage of the Variational Method is that no discretization error is introduced, as in the finite difference case, and the convergence of the results depends only on how many quantum numbers are taken. Just to have a comparison, we have taken a SiNW with cross-section $L_x = L_y = 10$ nm, and we have evaluated the eigenvalues with the two methods. In the figure 1 we plot the first ten eigenvalues ε_α obtained with the finite difference scheme, by increasing the grid points $N_g = N_1 = N_2$. From this figure we can clearly see that the convergence is reached for N_g= 141. In such a case, the matrix dimension is 19881 × 19881 and the CPU time was $\simeq$ 19000 sec (using MATLAB and an AMD Phenom II X6 1090T processor). If we want to obtain a similar result with the Variational Method, we have to take into account $N_x = N_y = 16$ quantum numbers. In this case the matrix dimension is 289 × 289 and the CPU time was $\simeq$ 163 sec. The percentage error between the two methods is shown in the figure 2. Similar errors are obtained for the envelope functions.

4 Ballistic transport

Once the quantum confinement in the transversal cross-section of the wire has been dealt with by efficiently solving the EMA equation, another issue is the description of the charge transport in the longitudinal direction of the nanowire. If the channel size of the device is far larger than the scattering length, carriers undergo a large number of

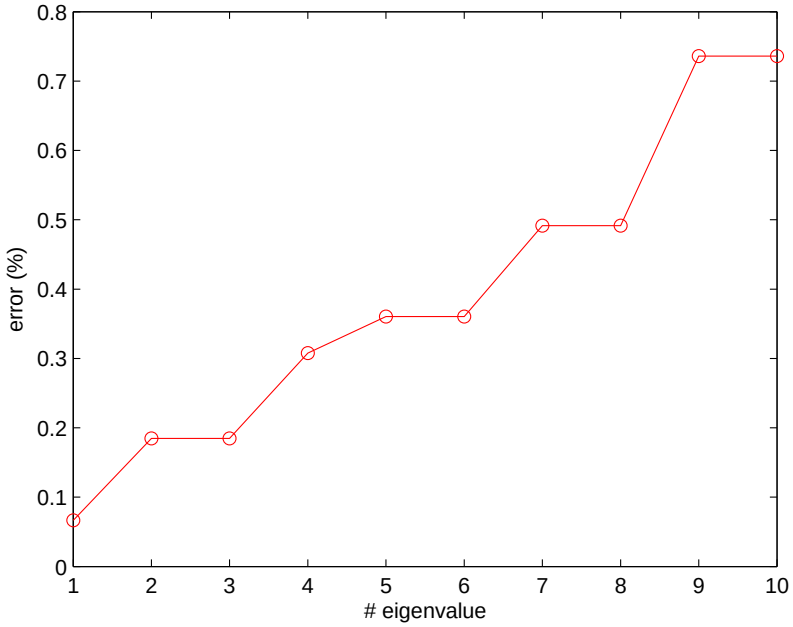

Figure 2: The percentage error between the subband energies ε_α (4) obtained with a finite difference solver and the Variational Method.

scattering processes which result in the diffusive carrier motion. If the channel device size is further decreased to less than the scattering length, ballistic carrier motion dominates the transport. The upper limit of the channel size to have a ballistic regime is an open question. Experimental results obtained in deeply scaled silicon MOSFETs [21] have shown that the carrier transport is near ballistic for channel sizes lesser than 50 nm.

In this paper we have considered the optimistic case of fully ballistic transport. The electrons are in equilibrium with their injecting reservoir (source or drain) which adsorbs and feed carriers into the channel without reflections. The charges are injected into the channel with unity probability, if their energy in the longitudinal direction is larger than the maximum subband energy $\varepsilon_{\alpha z}$. Then the carriers are transferred from the source to the drain without being scattered, and by neglecting tunneling effects. The source-to-drain current I can be evaluated with use of the method proposed in Landauer's formula [22], which is expressed as a sum of many one-dimensional subband components. Each subband current component flowing in one direction is given by the product of the unit charge, the number of carriers flowing into the subband per unit time, the transmission coefficient of the subband, all integrated over the carrier energy. The number of carriers flowing into the subband is further expressed by the product of the input carrier group velocity, the density of states, and the probability that the state is occupied by the carrier. In the not-degenerate case, the probability of carrier occupancy is given by the maxwellian distribution function with the source Fermi level on the source side, and that with the

drain Fermi level on the drain side of the subband. Both current directions, the one from the source to the drain and that in the opposite direction, should be considered. Then we have

$$I = q \sum_{\alpha} \int_0^{+\infty} v D(E_\alpha) \left\{ f_\alpha^{(eq)}(E_\alpha, E_{FS}) - f_\alpha^{(eq)}(E_\alpha, E_{FD}) \right\} T(E_\alpha)\, dE_\alpha \tag{16}$$

where $v = \hbar k_z / m^*$ is the group velocity, and $D_\alpha(E_\alpha)$ is the one-dimensional density of state

$$D(E_\alpha) = \frac{\sqrt{2m^*}}{\hbar \pi} \frac{\Theta(E_\alpha - \varepsilon_{\alpha z})}{\sqrt{E_\alpha - \varepsilon_{\alpha z}}} \quad . \tag{17}$$

$T(E_\alpha)$ is the subband transmission coefficient which, in the ballistic transport, implies

$$T(E_\alpha) = \begin{cases} 1 \quad \text{if} \quad E_\alpha \geq \varepsilon_\alpha^{Max} = \max_z \varepsilon_{\alpha z} \\ 0 \quad \text{otherwise} \end{cases} \tag{18}$$

In the not-degenerate case the equilibrium distribution function is the maxwellian, i.e.

$$f_\alpha^{(eq)}(E_\alpha, E_F) \propto \exp\left(-\frac{E_\alpha - E_F}{k_B T} \right) \tag{19}$$

where E_F is the Fermi energy and T the lattice temperature. E_{FS}, E_{FD} are the source and the drain Fermi energies respectively. If V_D and V_S are the applied voltage biases at the drain and source respectively, $V_{DS} = V_D - V_S$ then $E_{FD} = E_{FS} - qV_{DS}$.

The Fermi energy is obtained by imposing charge neutrality along each cross-section of the device, i.e.

$$\int\int n^{(eq)}(x, y, z)\, dx\, dy = \int\int (N_D - N_A)\, dx\, dy \tag{20}$$

and, if we suppose that the doping depends only on the longitudinal dimension z, we obtain

$$E_F(z) = -k_B T \log \left\{ \frac{\sqrt{2m^* k_B T}}{\pi \hbar \left[N_D(z) - N_A(z) \right] L_x L_y} \sum_{\alpha} \exp\left(-\frac{\varepsilon_{\alpha z}}{k_B T} \right) \right\} \quad . \tag{21}$$

The equilibrium linear electron density (7) is evaluated using eqs.17),(19),(21)

$$\rho_\alpha^{(eq)}(z) = \int D_\alpha(E_{\alpha z}) f_\alpha^{(eq)}\, dE_{\alpha z} = (N_D - N_A) L_x L_y \frac{\exp\left(-\frac{\varepsilon_{\alpha z}}{k_B T} \right)}{\sum_\alpha \exp\left(-\frac{\varepsilon_{\alpha z}}{k_B T} \right)} \quad . \tag{22}$$

Then by easy calculations eq.(16) reduces to

$$I = \frac{2q}{\hbar \pi} k_B T \sum_{\alpha} \exp\left(-\frac{\varepsilon_\alpha^{Max}}{k_B T} \right) \left\{ \exp\left(\frac{E_{FS}}{k_B T} \right) - \exp\left(\frac{E_{FD}}{k_B T} \right) \right\} \quad . \tag{23}$$

5 Simulation of a triple-gate SiNW transistor

We have considered a SiNW transistor with a parallelepiped shape, having square cross-section with dimension $L_x = L_y = 10$ nm and longitudinal dimension (i.e. the free transport direction) $L_z = 120$ nm. The device consists in an internal parallelepiped filled by Si (having dimension 8 x 8 nm^2) surrounded by SiO_2 of 1 nm thickness, producing the confining potential (14). The silicon, in the internal parallelepiped, is doped in the n^+ region with $N_D^+ = 10^{18}\,\mathrm{cm}^{-3}$ and in the n region with $N_D = 10^{16}\,\mathrm{cm}^{-3}$, with a regularization at the two junctions given by a hyperbolic tangent profile, i.e.

$$N_D(z) = N_D^+ - \frac{N_D^+ - N_D^-}{2}\left[\tanh\left(\frac{z-z_1}{s}\right) - \tanh\left(\frac{z-z_2}{s}\right)\right] \tag{24}$$

where $s = 5$ nm and $z_1 = 10$ nm, $z_1 = 80$ nm. The bottom of the parallelepiped (for z=0) is the source contact, and the top (for $z = 120$ nm) the drain contact. The triple-gate contact surrounds three faces of the parallelepiped with an extension $20 \le z \le 100$ nm. The applied biases are V_S= 0, V_D= 0.5 V and V_G is considered variable. The simulation procedure is the following:

- the EMA equation (4) is solved with $V_{tot} = U$ in each cross-section (z = const.), obtaining the subband energies $\varepsilon_{\alpha z}$ and envelope functions $\chi_{\alpha z}$.
- These functions are used to evaluate the charge density (6) in equilibrium condition, i.e. with ρ_α given by eq.(22).
- The Poisson equation (5) is solved leading to a new $V_{tot} = U - e\Phi$.
- If the new V_{tot} does not coincide sufficiently well with the old one, we start a further loop by solving the EMA equation with the new confining potential until the maximum difference between these two quantities is smaller than a predetermined tolerance.
- For each α-th subband, we evaluate $\varepsilon_\alpha^{Max} = \max_z \varepsilon_{\alpha z}$, and finally the current (23) is obtained.

We have taken into account only the first four subbands ($\alpha = 1, 2, 3, 4$) since, numerical experiments, shown that the other ones are very scarcely populated. The simulation results are shown in the figure 3. This characteristic curve, obtained in the ballistic approximation, gives us an upper limit to the the performance of this device, and the chosen approximations ensure a very good trade off between accuracy and computational resources required. Further extensions, such as including a more sophisticated transport model per subband according to the guidelines in [23]-[29], is under current investigations and will be presented in the next future.

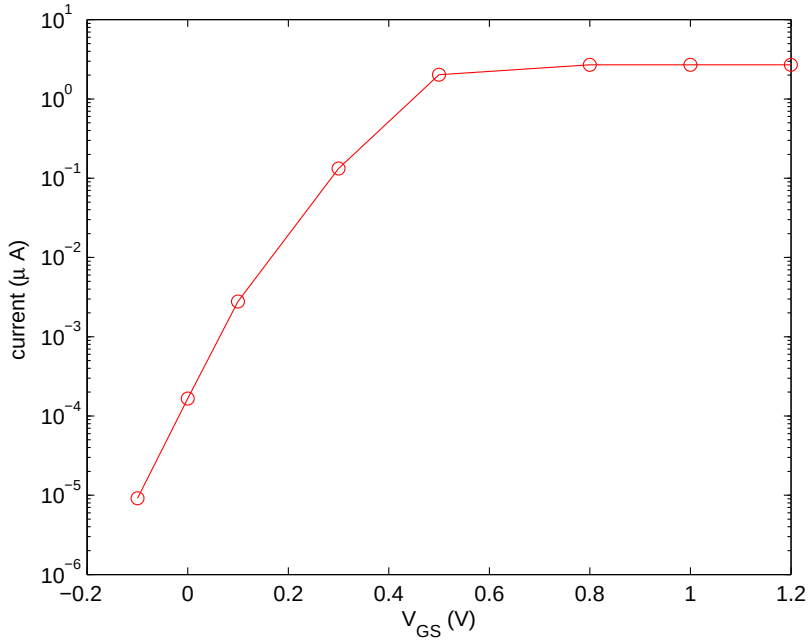

Figure 3: The current (23) versus the gate voltage V_{GS}.

Acknowledgment

We acknowledge the support of the Università degli Studi di Catania, FIR 2014 "Charge Transport in Graphene and Low dimensional Structures: modeling and simulation".

REFERENCES

[1] Ferry, D.K. Goodnick, S.M. and Bird, J. *Transport in nanostructures*. Cambridge University Press, (2009).

[2] Ramayya, E.B. Vasileska, D. Goodnick, S.M. and Knezevic, I. Electron mobility in Silicon Nanowires. *IEEE Trans. Nanotech.* (2007) **6**(1):113-117

[3] Ramayya, E.B. Vasileska, D. Goodnick, S.M. and Knezevic, I. Electron transport in silicon nanowires: The role of acoustic phonon confinement and surface roughness scattering. *J. Appl. Physics* (2008) **104**:063711.

[4] Ramayya, E.B. and Knezevic, I. Self-consistent Poisson-Schrödinger-Monte Carlo solver: electron mobility in silicon nanowires. *J. Comput. Electron.* (2010) **9**:206-210.

[5] Aksamija, Z. and Knezevic, I. Thermoelectric properties of silicon nanostructures, *J. Comput. Electron.* (2010) **9**: 173-179.

[6] Muscato, O. Monte Carlo evaluation of the transport coefficients in a n+ - n - n+ silicon diode. *COMPEL* (2000) **19**(3): 812-828.

[7] Muscato, O. and Wagner, W. Time step truncation in direct simulation Monte Carlo for semiconductors. *COMPEL* (2005) **24**(4): 1351-1366.

[8] Muscato, O. Wagner, W. and Di Stefano, V. Numerical study of the systematic error in Monte Carlo schemes for semiconductors. *ESAIM: M2AN* (2010) **44**(5): 1049-1068.

[9] Muscato, O. Wagner, W. and Di Stefano, V. Properties of the steady state distribution of electrons in semiconductors. *Kinetic and Related Models* (2011) **4**(3): 809-829.

[10] Muscato, O. Di Stefano, V. and Wagner, W. A variance-reduced electrothermal Monte Carlo method for semiconductor device simulation. *Computers & Mathematics with Applications* (2013) **65**(3):520-527.

[11] Lenzi, M.L. Palestri, P. Gnani, E. Gnudi A., Esseni, D. Selmi, L. and Baccarani, G. Investigation of the transport properties of silicon nanowires using deterministic and Monte Carlo approaches to the solution of the Boltzmann transport equation. *IEEE Trans. Electr. Dev.* (2008) **55**(8):2086-2096

[12] Ossig, G. and Schuerrer, F. Simulation of non-equilibrium electron transport in silicon quantum wires. *J. Comput. Electron.* (2008) **7**: 367-370.

[13] Majorana, A. Muscato, O. and Milazzo, C. Charge transport in 1D silicon devices via Monte Carlo simulation and Boltzmann-Poisson solver. *COMPEL* (2004) **23**(2): 410-425.

[14] Muscato O. and Di Stefano V., Hydrodynamic modeling of silicon quantum wires. *J. Comp. Electr.* (2012) **11**:45-55

[15] Muscato O. and Di Stefano V., Coupled quantum-classical transport in silicon nanowires. In: S. Idelsohn, M. Papadrakakis and B. Schrefler. Computational Methods for Coupled Problems in Science and Engineering V. p. 1109-1119, BARCELONA:CIMNE (Int. Center for Num. Meth. in Engineering), ISBN: 978-84-941407-6-1, Ibiza, 17-19 June 2013

[16] Muscato O. and Di Stefano V., Electro-thermal behaviour of a sub-micron silicon diode, *Semicond. Sci. Technol.* (2013) **28**: 025021

[17] Muscato O. and Di Stefano V., Hydrodynamic simulation of a n+ - n - n+ silicon nanowire, *Contin. Mech. Thermodyn.* (2014) **26**:197-205

[18] Muscato, O. Pidatella, R.M. and Fischetti, M.V. Monte Carlo and hydrodynamic simulation of a one dimensional $n^+ - n - n^+$ silicon diode. *VLSI Design* (1998) **6**(1-4): 247-250.

[19] Potter D., *Computational Physics*. Wiley, (1972).

[20] Suzuki Y. and Varga K., *Stochastic Variational Approach to Quantum-Mechanical Few Body Problems*. Springer, (1998).

[21] Lochtefeld A. and Antoniadis D.A., On Experimental Determination of Carrier Velocity in Deeply Scaled NMOS: How Close to the Thermal Limit?, *IEEE ELEC. DEV. LETTERS* (2001) **22**(2):95-97

[22] Natori K., Ballistic metal-oxide-semiconductor field effect transistor, *J. Appl. Phys.* (1994) **76**(8):4879-4890

[23] Muscato, O. and Di Stefano, V. Modeling heat generation in a sub-micrometric $n^+ - n - n^+$ silicon diode. *J. Appl. Phys.* (2008) **104**(12): 124501.

[24] Muscato, O. and Di Stefano, V. Hydrodynamic modeling of the electro-thermal transport in silicon semiconductors. *J. Phys. A: Math. Theor.* (2011) **44**(10): 105501.

[25] Muscato, O. and Di Stefano, V. An Energy Transport Model Describing Heat Generation and Conduction in Silicon Semiconductors. *J. Stat. Phys.* (2011) **144**(1): 171-197.

[26] Muscato, O. and Di Stefano, V. Local equilibrium and off-equilibrium thermoelectric effects in silicon semiconductors. *J. Appl. Phys.* (2011) **110**(9): 093706.

[27] Muscato, O. and Di Stefano, V. Heat generation and transport in nanoscale semiconductor devices via Monte Carlo and hydrodynamic simulations. *COMPEL* (2011) **30**(2): 519-537.

[28] Di Stefano, V. and Muscato, O. Seebeck Effect in Silicon Semiconductors. *Acta Appl. Math.* (2012) **122**(1): 225-238.

[29] Davoody, A.H. Ramayya, E.B. Maurer, L.N. and Knezevic, I. Ultrathin GaN nanowires: Electronic, thermal, and thermoelectric properties. *Phys. Rev. B* (2014) **89**(11):115313